General Sensitivity Formulas for Maximum Loading Conditions in Power Systems

F. Milano, A. J. Conejo and R. Zárate-Miñano

Department of Electrical Engineering

University of Castilla-La Mancha, Ciudad Real, Spain

Abstract

This paper proposes general sensitivity formulas for maximum loading conditions of nonlinear power systems. The proposed formulas allow computing the sensitivities of any system variable and, in particular, of the maximum loading margin with respect to arbitrary parameters. This approach extends previous results. The paper also shows that the sensitivity formulas available in the literature for static saddle-node and limit-induced bifurcation points are particular cases of the proposed general formulas. Two benchmark systems, namely a 6-bus system and the IEEE RTS-96 24-bus tests system, are used to illustrate and test the proposed technique.

List of symbols

The main notation used throughout the paper is stated below for quick reference. In the paper, vectors and matrices are in bold face, while scalar variables are in italic font (e.g. $\boldsymbol{v}$ is the vector of voltage magnitudes v_i at each bus i). Other symbols are defined as required in the text.

Functions

$f(\cdot)$ The optimal power flow objective function.

$\boldsymbol{h}(\cdot)$ Vector of equality constraints.

$\hat{\boldsymbol{h}}(\cdot)$ Extended vector of equality constraints.

$\boldsymbol{g}(\cdot)$ Vector of inequality constraints.

$\mathcal{L}(\cdot)$ The Lagrangian function.

Variables

v_i Voltage magnitude at bus i.

θ_i Voltage angle at bus i.

k_G Variable used to distribute the system losses among generators.

q_{Gi} Generator reactive power at bus i.

ψ_k Current flow in transmission line k.

Other Variables ("outside" the OPF Problem)

p_{Gi}^{λ} total generation power injected at bus i.

p_{Li}^{λ} total load power consumed at bus i.

Multipliers

$\boldsymbol{\pi}$ Lagrangian multipliers of equalities $\boldsymbol{h}$.

$\hat{\boldsymbol{\pi}}$ Lagrangian multipliers of equalities $\hat{\boldsymbol{h}}$.

$\boldsymbol{\mu}$ Lagrangian multipliers of inequalities $\boldsymbol{g}$.

Constants

p_{Gi} Generated active power at bus i.

p_{Li} Load active power at bus i.

q_{Li} Load reactive power at bus i.

ϕ_{Li} Load power factor at bus i.

Sets

J Set of active inequality constraints.

J_d Set of degenerate inequality constraints.

Numbers

n Number of power flow variables.

ℓ Number of equality constraints.

m Number of inequality constraints.

p Number of parameters.

m_J Cardinality of J, i.e., the number of active inequality constraints.

n_B Number of buses.

n_L Number of lines.

Indices

i, ι Indices for buses.

l Indices for equality constraints.

j Indices for active inequality constraints.

k Indices for lines.

1 Introduction

The maximum loading condition of a power system is of particular interest for technical and economical reasons. As a consequence, a variety of techniques

and studies have been proposed in order to compute the loading margin of a system or the distance of an operating point to collapse [1–3]. This paper focuses on collapse phenomena driven by static saddle-node and limit-induced bifurcations [4–6].

One of the first techniques used to determine the maximum loading condition of a power system was the continuation power flow (CPF) [7]. This technique consists of computing a series of power flows while increasing the overall loading level of the system. The CPF is shown to be robust even for solutions close to the collapse point, which is typically a *critical* point from both the physical (blackout) and numerical (singularity of equations) point of view [3].

It can also be demonstrated that the CPF analysis, if used for determining the maximum loading condition, is a gradient reduced method [8]. This notable fact has been exploited to use optimization methods rather than the CPF analysis. The first OPF problem for computing the reactive power margin with respect to voltage collapse was formulated in [9]. A variety of stability constrained OPF problems have been proposed in [10–12]. In particular, [12] shows that the stability constrained OPF problem is also suitable for studying the effect of the loadability of the network on the market clearing procedure.

The computation of the maximum loading condition is only a part of the information that can be useful to avoid instability. One can be interested in determining how the parameters of the system affects the loading margins [13]. This is useful both to determine the most critical parameters and to

design an effective corrective action to avoid the collapse [14].

This information can be obtained by a sensitivity analysis at the maximum loading condition. All sensitivity methods for the maximum loading condition problem that have been proposed in the literature are based on the linearization of the system equations at the critical point [14, 15, 21], or on CPF-based numerical analyses [16].

It has to be noted the relevance of the sensitivity analysis in several practical applications. For example, in [17], [18] and [19], a sensitivity analysis is carried out to define the most critical contingency, while in [20] and [16], to properly set up primary and secondary voltage regulation, respectively. In [18], the sensitivities are used as economic signals for market participants. In [21], the sensitivities are used to determine the most efficient remedial actions for strengthening systems subjected to load increases and/or contingencies. Finally sensitivities are effective tools for determining the reactive power compensation and for sizing FACTS [22].

This paper provides generalized sensitivity expressions based on the solution of a voltage stability constrained OPF . These expressions use the dual variables (Lagrangian multipliers) at the optimal solution and the properties of the KKT optimality conditions [23–25]. In this paper, the theory that was proposed in [24] is applied to the maximum loading condition problem. As a byproduct, it can be demonstrated that the general sensitivity formulas that are proposed in this paper can be reduced to the formulas for saddle-node bifurcation and limit-induced bifurcation given in [20].

In summary, the novel contributions of this paper are:

1. General expression of sensitivities of a generic OPF variable with respect to a generic parameter.

2. Specific sensitivities of the loading margin at the maximum loading condition with respect to arbitrary parameters.

3. Unique and close expressions of sensitivities at saddle-node and limit-induced bifurcation points.

2 OPF-based Maximum Loading Condition Problem

In this paper, the following general optimization problem is used to represent a maximum loading condition problem, based on what has been proposed in [13]:

$$\begin{array}{c} \text{Minimize} \\ \boldsymbol{x}, \ \lambda \\ z = f(\boldsymbol{x}, \lambda, \boldsymbol{a}) \end{array} \tag{1}$$

subject to

$$\boldsymbol{h}(\boldsymbol{x}, \lambda, \boldsymbol{a}) = \boldsymbol{0} : \boldsymbol{\pi} \tag{2}$$

$$\boldsymbol{g}(\boldsymbol{x}, \lambda, \boldsymbol{a}) \leq \boldsymbol{0} : \boldsymbol{\mu} , \tag{3}$$

where the vector $\boldsymbol{x} \in \mathbb{R}^n$ and the loading margin $\lambda \in \mathbb{R}$ are the variables, the vector $\boldsymbol{a} \in \mathbb{R}^p$ are the parameters, and $\boldsymbol{h}(\boldsymbol{x}, \boldsymbol{a}) = (h_1(\boldsymbol{x}, \boldsymbol{a}), \dots, h_\ell(\boldsymbol{x}, \boldsymbol{a}))^T$

and $\boldsymbol{g}(\boldsymbol{x}, \boldsymbol{a}) = (g_1(\boldsymbol{x}, \boldsymbol{a}), \ldots, g_m(\boldsymbol{x}, \boldsymbol{a}))^T$ are the equality and inequality constraints, respectively. Vector $\boldsymbol{x}$ includes all optimization variables (e.g. bus voltages), while $\boldsymbol{\pi}$ and $\boldsymbol{\mu}$ are the Lagrange multiplier vectors for equality and inequality constraints, respectively. The parameter vector $\boldsymbol{a}$ includes, for example, generator and load powers ($\boldsymbol{p}_G$ and $\boldsymbol{p}_L$, respectively), line resistances ($R_{i\iota}$), reactances ($X_{i\iota}$), and susceptances (B_i); load power factors; generator reactive power limits; and voltage limits. The objective function and the equality and inequality constraints in (1)-(3) are defined below.

2.1 Objective function

The objective function used in this paper is:

$$z = -\lambda . \tag{4}$$

Minimizing $-\lambda$ corresponds to find the maximum loading condition that can be either associated with [3]:

1. voltage stability limit (collapse point) corresponding to a system singularity (saddle-node bifurcation);

2. system controller limits like generator reactive power limits (limit-induced bifurcation).

3. thermal or bus voltage limit.

Observe that (4) is the simplest objective function that allows taking into account voltage stability constraints. Other more sophisticated models have

been proposed in [10] and [12]. Nevertheless, the main goal of this paper is to formulate a general expression of sensitivity formulas of the loading margin λ with respect to an arbitrary parameter. The conclusions to be drawn using (4) can thus be easily extended to other objective functions and OPF models of the form (1)-(3).

2.2 Equality constraints

The set $\boldsymbol{h}$ ($\boldsymbol{h} : \mathbb{R}^{n+m} \to \mathbb{R}^{\ell}$) represents the algebraic equations of the system. According to typical assumptions in voltage stability studies [3], loads are assumed to have constant power factor, thus:

$$q_{Li} = \tan(\phi_{Li})p_{Li} \qquad \forall i = 1, \ldots, n_B \ . \tag{5}$$

Furthermore, the loading margin λ increases generator and load powers as follows:

$$
\begin{aligned}
p_{Gi}^{\lambda} &= (\lambda + k_G)\, p_{Gi} \qquad \forall i = 1, \ldots, n_B \\
p_{Li}^{\lambda} &= \lambda\, p_{Li} \qquad \forall i = 1, \ldots, n_B \ .
\end{aligned}
\tag{6}
$$

The total power injections and consumptions $\boldsymbol{p}_G^{\lambda}$ and $\boldsymbol{p}_L^{\lambda}$ are not explicitly defined in (1)-(3), thus they are not included in $\boldsymbol{x}$. Note that variable k_G allows distributing losses corresponding to the loading level defined by λ among all generators. Other possible mechanisms to handle increasing losses could be implemented, but they are beyond the scope of this paper.

2.3   Inequality constraints

In (1)-(3), the set of inequality constraints $\boldsymbol{g}$ represents the physical and security limits of the system.

The physical and security limits considered in this paper are similar to those proposed in [26], and take into account transmission line thermal limits:

$$\psi_k \leq \psi_k^{\max} \qquad \forall k = 1, \dots, n_L \ , \tag{7}$$

generator reactive power limits:

$$q_{Gi}^{\min} \leq q_{Gi} \leq q_{Gi}^{\max} \qquad \forall i = 1, \dots, n_B \ , \tag{8}$$

and voltage magnitude limits:

$$v_i^{\min} \leq v_i \leq v_i^{\max} \qquad \forall i = 1, \dots, n_B \ . \tag{9}$$

2.4   Non-degenerate and Degenerate Optimal Solution Points

It is noteworthy to observe that problem (1)-(3) presents $n+1$ variables, i.e. $(\boldsymbol{x}, \lambda)$, while the number of equality constraints $\boldsymbol{h}$ is ℓ. Thus, at the optimal solution, only up to $n+1-\ell$ inequality constraints g_j can be binding and non-degenerate at a time.[1] If more than $n+1-\ell$ inequality constraints are binding, say m_J, $m_{Jd} = (m_J - n - 1 + \ell)$ constraints will be degenerate. However, the case with degenerate constraints can be easily taken into account, as explained in Section 3.1.

---

[1]A *degenerate* constraint is a binding inequality constraint with associated null multiplier. For a rigorous definition of *degenerate inequality constraints* please refer to [27].

In the OPF notation, active inequality constraints can be expressed as

$$g_j(\tilde{\boldsymbol{x}}, \tilde{\lambda}, \boldsymbol{p}) = 0 \quad j = 1, \ldots, m_J \, . \tag{10}$$

Since only $n + 1 - \ell$ of the m_J constraint is non-degenerate, there will be m_{Jd} inequality constraints that are redundant and can be removed from problem (1)-(3). This also implies that m_{Jd} dual variables associated to m_{Jd} active inequality constraints will be equal to zero.

3   Sensitivity Analysis

In addition to the optimal operating point, the solution of the OPF-based maximum loading condition problem (1)-(3) provides a set of relevant sensitivities.

Section 3.1 provides general sensitivity expressions of a generic variable with respect to an arbitrary parameter of the system. General formulas are particularized for the case of the sensitivity of the loading margin λ with respect to an arbitrary parameter in Section 3.2. Finally, in Section 3.3, sensitivities at bifurcation points are developed.

3.1   General Sensitivity Expressions

Associated with problem (1)-(3) is the Lagrangian function

$$\mathcal{L} = f(\boldsymbol{x}, \lambda, \boldsymbol{a}) + \boldsymbol{\pi}^T \boldsymbol{h}(\boldsymbol{x}, \lambda, \boldsymbol{a}) + \boldsymbol{\mu}^T \boldsymbol{g}(\boldsymbol{x}, \lambda, \boldsymbol{a}) \, . \tag{11}$$

In the following it is assumed that problem (1)-(3) has an optimal solution

$\boldsymbol{x}^*$, λ^*, $\boldsymbol{a}$, $\boldsymbol{\pi}^*$, $\boldsymbol{\mu}^*$, z^*. To obtain sensitivity equations, the feasible solution is perturbed in such a way that the KKT conditions still hold [24].

The expressions of the sensitivities of a generic variable with respect to the parameters are as follows. Assuming that the problem (1)-(3) is regular (see [27] or [28]) and using the results reported in [23–25], a feasible perturbation leads to the following linear system of equations:

$$
\begin{bmatrix}
\boldsymbol{F_x} & \boldsymbol{F_\lambda} & \boldsymbol{F_a} & \boldsymbol{0} & \boldsymbol{0} & -1 \\
\boldsymbol{F_{xx}} & \boldsymbol{F_{x\lambda}} & \boldsymbol{F_{xa}} & \boldsymbol{H_x^T} & \boldsymbol{G_x^T} & 0 \\
\boldsymbol{F_{\lambda x}} & \boldsymbol{F_{\lambda\lambda}} & \boldsymbol{F_{\lambda a}} & \boldsymbol{H_\lambda^T} & \boldsymbol{G_\lambda^T} & 0 \\
\boldsymbol{H_x} & \boldsymbol{H_\lambda} & \boldsymbol{H_a} & \boldsymbol{0} & \boldsymbol{0} & 0 \\
\boldsymbol{G_x} & \boldsymbol{G_\lambda} & \boldsymbol{G_a} & \boldsymbol{0} & \boldsymbol{0} & 0
\end{bmatrix}
\begin{bmatrix}
d\boldsymbol{x} \\
d\lambda \\
d\boldsymbol{a} \\
d\boldsymbol{\pi} \\
d\boldsymbol{\mu} \\
dz
\end{bmatrix}
= \boldsymbol{0} \ ,
\tag{12}
$$

where all vectors and sub-matrices are defined in the Appendix. It is important to note that sub-matrices $\boldsymbol{G_x}$, $\boldsymbol{G_\lambda}$ and $\boldsymbol{G_a}$ are built by removing from $\boldsymbol{g}$ all degenerate constraints. This operation does not imply additional computations, as degenerate constraints are active constraints with null Lagrangian multipliers.

Observe that for problem (1)-(3), the number of equality constraints plus the maximum number of inequalities constraints that can be active and non-degenerate is equal to the dimension of $(\boldsymbol{x}, \lambda)$, i.e. $\ell + m_J = n + 1$,[2] as discussed in Section 2.4. Observe that the sub-matrix, say $\mathcal{H_x}$, obtained by removing one row from the the matrix $[\boldsymbol{H_x^T}, \boldsymbol{G_x^T}]^T$, is square. This property is important as in Subsection 3.2.2 we use the fact that $\mathcal{H_x}$ is invertible.

To compute sensitivities with respect to the components of the parameter

---

[2]Observe that $\ell + m_J = n$, i.e. $\ell + m_J < n + 1$, in the case of SNB points.

vector $\boldsymbol{a}$, system (12) can be written as

$$\boldsymbol{U} \begin{bmatrix} d\boldsymbol{x} & d\lambda & d\boldsymbol{\pi} & d\boldsymbol{\mu} & dz \end{bmatrix}^T = \boldsymbol{S}\, d\boldsymbol{a}, \tag{13}$$

where the matrices $\boldsymbol{U}$ and $\boldsymbol{S}$ are respectively

$$\boldsymbol{U} = \left[\begin{array}{c|c|c|c|c} \boldsymbol{F_x} & \boldsymbol{F_\lambda} & \boldsymbol{0} & \boldsymbol{0} & -1 \\ \hline \boldsymbol{F_{xx}} & \boldsymbol{F_{x\lambda}} & \boldsymbol{H_x^T} & \boldsymbol{G_x^T} & 0 \\ \hline \boldsymbol{F_{\lambda x}} & \boldsymbol{F_{\lambda\lambda}} & \boldsymbol{H_\lambda^T} & \boldsymbol{G_\lambda^T} & 0 \\ \hline \boldsymbol{H_x} & \boldsymbol{H_\lambda} & \boldsymbol{0} & \boldsymbol{0} & 0 \\ \hline \boldsymbol{G_x} & \boldsymbol{G_\lambda} & \boldsymbol{0} & \boldsymbol{0} & 0 \end{array} \right] \tag{14}$$

$$\boldsymbol{S}^T = -\begin{bmatrix} \boldsymbol{F_a} & \boldsymbol{F_{xa}} & \boldsymbol{F_{\lambda a}} & \boldsymbol{H_a} & \boldsymbol{G_a} \end{bmatrix} \tag{15}$$

and therefore

$$\begin{bmatrix} d\boldsymbol{x} & d\lambda & d\boldsymbol{\pi} & d\boldsymbol{\mu} & dz \end{bmatrix}^T = \boldsymbol{U}^{-1}\boldsymbol{S}\, d\boldsymbol{a}. \tag{16}$$

Replacing $d\boldsymbol{a}$ by the p-dimensional identity matrix $\boldsymbol{I}$ in (16) all the derivatives are obtained. Thus, the matrix with all derivatives with respect to parameters becomes

$$\begin{bmatrix} \dfrac{d\boldsymbol{x}}{d\boldsymbol{a}} & \dfrac{d\lambda}{d\boldsymbol{a}} & \dfrac{d\boldsymbol{\pi}}{d\boldsymbol{a}} & \dfrac{d\boldsymbol{\mu}}{d\boldsymbol{a}} & \dfrac{dz}{d\boldsymbol{a}} \end{bmatrix}^T = \boldsymbol{U}^{-1}\boldsymbol{S}. \tag{17}$$

Expression (17) allows deriving sensitivities of the variables, the multipliers (dual variables) and the objective function with respect to all parameters. Therefore, the sensitivities of the loading margin and other system variables with respect to power supplies and demands are straightforwardly obtained using expression (17).

The computational complexity of building and inverting matrices $\boldsymbol{U}$ and $\boldsymbol{S}$ and evaluating expression (17) is moderate even for large scale electric energy systems, as explained below.

1. The computation of the submatrices that form U is a required step to solve the OPF problem, thus these matrices are available for the sensitivity analysis. Finally, the computation of the inverse of U is not particularly costly because U is typically highly sparse.

2. The computation and the time required for computing S depends on the parameter vector a that has been selected for the sensitivity analysis. For example, in case a includes just load powers, S is a matrix of zeros and ones.

It should be noted that matrix U is generally invertible because the solution is regular and because all degenerate constraints (if any) have been removed for building matrix (12). However, if it is not, alternative procedures (more computationally involved) to obtain and/or analyze the sensitivities are available [24].

3.2 Specific Sensitivity Expressions

This section focuses on a subset of the general formulas (17), namely the sensitivities of the loading margin with respect to parameters a. These sensitivities have a particular relevance in the literature [15], [21] and [20]. Sensitivities of other variables obtained using (17) are illustrated in Section 4.

Equations (17) include $d\lambda/da$. However, for the sake of derivation, $d\lambda/da$ are derived in this section from applying the KKT conditions to (11), as follows.

The KKT conditions with respect to system variables $\boldsymbol{x}$ and λ are:

$$\nabla_{\boldsymbol{x}}\mathcal{L} = \boldsymbol{F_x} + [\boldsymbol{\pi^*}]^T\boldsymbol{H_x} + [\boldsymbol{\mu^*}]^T\boldsymbol{G_x} = \boldsymbol{0} \tag{18}$$

$$\nabla_{\lambda}\mathcal{L} = \boldsymbol{F_\lambda} + [\boldsymbol{\pi^*}]^T\boldsymbol{H_\lambda} + [\boldsymbol{\mu^*}]^T\boldsymbol{G_\lambda} = 0 , \tag{19}$$

where all Jacobian matrices with respect to $\boldsymbol{x}$ and λ are defined in the Appendix. By taking into account that $f = -\lambda$ in problem (1)-(3), one can rewrite (18) and (19) as follows:

$$\boldsymbol{0} = [\boldsymbol{\pi^*}]^T\boldsymbol{H_x} + [\boldsymbol{\mu^*}]^T\boldsymbol{G_x} \tag{20}$$

$$1 = [\boldsymbol{\pi^*}]^T\boldsymbol{H_\lambda} + [\boldsymbol{\mu^*}]^T\boldsymbol{G_\lambda} . \tag{21}$$

Furthermore, a feasible perturbation of equality and inequality constraints at the optimal point leads to the following expressions:

$$\boldsymbol{H_x}d\boldsymbol{x} + \boldsymbol{H_\lambda}d\lambda + \boldsymbol{H_a}d\boldsymbol{a} = \boldsymbol{0} \tag{22}$$

$$\boldsymbol{G_x}d\boldsymbol{x} + \boldsymbol{G_\lambda}d\lambda + \boldsymbol{G_a}d\boldsymbol{a} = \boldsymbol{0} , \tag{23}$$

where Jacobian matrices with respect to $\boldsymbol{a}$ are also defined in the Appendix and it is assumed that only non-degenerate binding constraints are considered in (23). Then, multiplying (22) and (23) by $[\boldsymbol{\pi^*}]^T$ and $[\boldsymbol{\mu^*}]^T$, respectively, gives:

$$[\boldsymbol{\pi^*}]^T\boldsymbol{H_x}d\boldsymbol{x} + [\boldsymbol{\pi^*}]^T\boldsymbol{H_\lambda}d\lambda + [\boldsymbol{\pi^*}]^T\boldsymbol{H_a}d\boldsymbol{a} = 0 \tag{24}$$

$$[\boldsymbol{\mu^*}]^T\boldsymbol{G_x}d\boldsymbol{x} + [\boldsymbol{\mu^*}]^T\boldsymbol{G_\lambda}d\lambda + [\boldsymbol{\mu^*}]^T\boldsymbol{G_a}d\boldsymbol{a} = 0 , \tag{25}$$

and adding (24) and (25) leads to:

$$([\boldsymbol{\pi^*}]^T\boldsymbol{H_x} + [\boldsymbol{\mu^*}]^T\boldsymbol{G_x})d\boldsymbol{x} + \tag{26}$$

$$([\boldsymbol{\pi^*}]^T\boldsymbol{H_\lambda} + [\boldsymbol{\mu^*}]^T\boldsymbol{G_\lambda})d\lambda +$$

$$([\boldsymbol{\pi^*}]^T\boldsymbol{H_a} + [\boldsymbol{\mu^*}]^T\boldsymbol{G_a})d\boldsymbol{a} = 0 .$$

Finally, substituting (20) and (21) in (26), one has:

$$d\lambda + ([\boldsymbol{\pi}^*]^T \boldsymbol{H_a} + [\boldsymbol{\mu}^*]^T \boldsymbol{G_a})d\boldsymbol{a} = 0 \ , \tag{27}$$

and thus the sensitivities of the loading margin λ with respect to parameters $\boldsymbol{a}$ are:

$$\frac{d\lambda}{d\boldsymbol{a}} = -[\boldsymbol{\pi}^*]^T \boldsymbol{H_a} - [\boldsymbol{\mu}^*]^T \boldsymbol{G_a} \ . \tag{28}$$

Note finally that (28) is a part of the general equations (17).

3.3   Sensitivity Formulas at Bifurcation Points

This section shows that general equations (28) are equivalent to the sensitivity formulas at the saddle-node bifurcation (SNB) and at the limit-induced bifurcation (LIB) given in [15]. In the context of optimization problems, SNBs and LIBs are regular optimal solutions. Thus a general expressions for sensitivities has to be expected.

For the sake of derivation, let us define the extended vector of equality constraints, say $\hat{\boldsymbol{h}}(\boldsymbol{x}^*, \lambda^*, \boldsymbol{a})$, as the vector of equations that is built using all equality constraints $\boldsymbol{h}$ and m_{Jd} binding non-degenerate inequality constraints. The Jacobian matrices of $\hat{\boldsymbol{h}}$ are as follows:

$$\begin{aligned}
\mathcal{H}_{\boldsymbol{x}} &= \nabla_{\boldsymbol{x}}\hat{\boldsymbol{h}}(\boldsymbol{x}^*, \lambda^*, \boldsymbol{a}) \tag{29} \\
\mathcal{H}_{\lambda} &= \nabla_{\lambda}\hat{\boldsymbol{h}}(\boldsymbol{x}^*, \lambda^*, \boldsymbol{a}) \\
\mathcal{H}_{\boldsymbol{a}} &= \nabla_{\boldsymbol{a}}\hat{\boldsymbol{h}}(\boldsymbol{x}^*, \lambda^*, \boldsymbol{a}) \ .
\end{aligned}$$

Observe that, as discussed in Section 3.1, $\mathcal{H}_{\boldsymbol{x}}$ is square.

3.3.1   Saddle-Node Bifurcations

Saddle-node bifurcations (SNBs) are characterized by a pair of equilibrium points coalescing and disappearing as the loading margin λ slowly changes. From the mathematical point of view, the SNB point is an equilibrium point $(\tilde{x}, \tilde{\lambda})$ with the following properties.

1. The Jacobian matrix $\mathcal{H}_{\boldsymbol{x}}$ is singular and has a simple and unique zero eigenvalue. Observe that even though $\mathcal{H}_{\boldsymbol{x}}$ is singular, the whole matrix $\boldsymbol{U}$ is non-singular, since the solution at the SNB is regular.

2. The right and left eigenvector $\boldsymbol{\nu}$ and $\boldsymbol{w}$, respectively, associated with the zero-eigenvalue are unique $(\mathcal{H}_{\boldsymbol{x}}\boldsymbol{\nu} = \mathcal{H}_{\boldsymbol{x}}^{T}\boldsymbol{w} = \boldsymbol{0})$.

3. The Jacobian matrix $\boldsymbol{w}^{T}\mathcal{H}_{\lambda} \neq \boldsymbol{0}$.

4. The last transversality condition is as follows: $\boldsymbol{w}^{T}[(\nabla_{x}^{2}\hat{\boldsymbol{h}})\boldsymbol{v}]\boldsymbol{v} \neq \boldsymbol{0}$.

A SNB point is a point for which the number of active non-degenerate inequalities is only $n - \ell$, not $n + 1 - \ell$. The maximum loading condition is given by the power flow equations that typically show a convex shape [2].

By taking the derivatives of $\boldsymbol{h}$ at the SNB point, one has:

$$\mathcal{H}_{\boldsymbol{x}}d\boldsymbol{x} + \mathcal{H}_{\lambda}d\lambda + \mathcal{H}_{\boldsymbol{a}}d\boldsymbol{a} = \boldsymbol{0} \tag{30}$$

$$\Rightarrow \boldsymbol{w}^{T}\mathcal{H}_{\boldsymbol{x}}d\boldsymbol{x} + \boldsymbol{w}^{T}\mathcal{H}_{\lambda}d\lambda + \boldsymbol{w}^{T}\mathcal{H}_{\boldsymbol{a}}d\boldsymbol{a} = 0 \ .$$

From these equations and given that $\boldsymbol{w}^{T}\mathcal{H}_{\boldsymbol{x}} = \boldsymbol{0}$ at the SNB point, one can obtain the sensitivities of the loading margin λ with respect to the parameters

$\boldsymbol{a}$ at the SNB point as proposed in [15]:

$$\frac{d\lambda}{d\boldsymbol{a}} = -\frac{\boldsymbol{w}^T \mathcal{H}_{\boldsymbol{a}}}{\boldsymbol{w}^T \mathcal{H}_\lambda} \ . \tag{31}$$

Moreover, it can be demonstrated that the following relationship holds at the SNB point [8]:

$$\boldsymbol{w} = \hat{\boldsymbol{\pi}}^* \ , \tag{32}$$

i.e., the left eigenvector $\boldsymbol{w}$ at the SNB point is equal to the Lagrangian multipliers $\hat{\boldsymbol{\pi}}^*$ of the power flow equations $\hat{\boldsymbol{h}}$. These Lagrangian multipliers include $n - \ell$ multipliers $\boldsymbol{\mu}^*$ associated with $n - \ell$ active non-degenerate inequality constraints $\boldsymbol{g}$ at the optimal point. Furthermore, from (11), one has that the derivatives of the Lagrangian function $\mathcal{L}$ with respect to the loading margin λ at the optimal point (x^*, λ^*) are:

$$\nabla_\lambda \mathcal{L} \quad = \quad -1 + [\hat{\boldsymbol{\pi}}^*]^T \mathcal{H}_\lambda = 0 \ , \tag{33}$$

where it has been used the fact that $\boldsymbol{F}_\lambda = -1$ and $\boldsymbol{G}_\lambda = \boldsymbol{0}$. Hence, one can easily see that (31), (32) and (33) lead to:

$$\frac{d\lambda}{d\boldsymbol{a}} = -\frac{\boldsymbol{w}^T \mathcal{H}_{\boldsymbol{a}}}{\boldsymbol{w}^T \mathcal{H}_\lambda} = -[\hat{\boldsymbol{\pi}}^*]^T \mathcal{H}_{\boldsymbol{a}} \tag{34}$$

and, since $\mathcal{H}_{\boldsymbol{a}}$ includes $n - \ell$ rows corresponding to active non-degenerate inequality constraints $\boldsymbol{g}$ at the optimal point, one finally obtains (28), as follows:

$$-[\hat{\boldsymbol{\pi}}^*]^T \mathcal{H}_{\boldsymbol{a}} = -[\boldsymbol{\pi}^*]^T \boldsymbol{H}_{\boldsymbol{a}} - [\boldsymbol{\mu}^*]^T \boldsymbol{G}_{\boldsymbol{a}} \ . \tag{35}$$

Observe that the SNB conditions ensure that $\boldsymbol{\pi}^*$ is not zero even if no limit is binding. However, (34) cannot take infinite values because of the transversality conditions of the SNB.

3.3.2   Limit-Induced Bifurcations

Limit-induced bifurcations (LIBs) are equilibrium points where a system control limit is reached. If the LIB implies a system collapse, it presents a pair of equilibrium points coalescing and disappearing for slow changes of the loading margin λ. However, as opposed to the SNB, at the LIB point the system Jacobian $\mathcal{H}_{\boldsymbol{x}}$ is not singular. In general, the LIB can be defined as follows:

$$\hat{\boldsymbol{h}}(\tilde{\boldsymbol{x}}, \tilde{\lambda}, \boldsymbol{a}) \;=\; \boldsymbol{0} \tag{36}$$
$$g_i(\tilde{\boldsymbol{x}}, \tilde{\lambda}, \boldsymbol{a}) \;=\; 0 \;,$$

where g_i is the remaining scalar binding and non-degenerate inequality constraint. Without lack of generality, it is assumed that all degenerate inequality constraints has been removed. Note that detecting degenerate constraints is straightforward as their associated dual variables are zero. The gradients of (36) are:

$$\mathcal{H}_{\boldsymbol{x}} d\boldsymbol{x} + \mathcal{H}_\lambda d\lambda + \mathcal{H}_{\boldsymbol{a}} d\boldsymbol{a} \;=\; \boldsymbol{0} \tag{37}$$
$$\boldsymbol{G}_{\boldsymbol{x}}^i d\boldsymbol{x} + \boldsymbol{G}_\lambda^i d\lambda + \boldsymbol{G}_{\boldsymbol{a}}^i d\boldsymbol{a} \;=\; 0 \;,$$

where $\boldsymbol{G}_{\boldsymbol{x}}^i$, $\boldsymbol{G}_\lambda^i$ and $\boldsymbol{G}_{\boldsymbol{a}}^i$ are the Jacobian matrices of g_i with respect to $\boldsymbol{x}$, λ and $\boldsymbol{a}$, respectively.

By eliminating $d\boldsymbol{x}$ from these equations, one has:

$$\frac{d\lambda}{d\boldsymbol{a}} = -\frac{\boldsymbol{G}_{\boldsymbol{a}}^i - \boldsymbol{G}_{\boldsymbol{x}}^i [\mathcal{H}_{\boldsymbol{x}}]^{-1} \mathcal{H}_{\boldsymbol{a}}}{\boldsymbol{G}_\lambda^i - \boldsymbol{G}_{\boldsymbol{x}}^i [\mathcal{H}_{\boldsymbol{x}}]^{-1} \mathcal{H}_\lambda} \;. \tag{38}$$

Furthermore the derivatives of the Lagrangian function $\mathcal{L}$ with respect to dependent variables in $\boldsymbol{x}$ at the maximum loading condition (x^*, λ^*) are,

from (11):

$$\nabla_{\boldsymbol{x}}\mathcal{L} \;=\; [\hat{\boldsymbol{\pi}}^*]^T\mathcal{H}_{\boldsymbol{x}} + [\mu_i^*]^T\boldsymbol{G}_{\boldsymbol{x}}^i = \boldsymbol{0}\;, \tag{39}$$

where $\hat{\boldsymbol{\pi}}^*$ are the Lagrangian multipliers of power flow equations $\hat{\boldsymbol{h}}$, and it has been used the fact that $\boldsymbol{F}_{\boldsymbol{x}} = \boldsymbol{0}$, as it can be deduced from the objective function of (1)-(3). Equation (39) leads to:

$$[\hat{\boldsymbol{\pi}}^*]^T = -\mu_i^*\boldsymbol{G}_{\boldsymbol{x}}^i[\mathcal{H}_{\boldsymbol{x}}]^{-1}\;, \tag{40}$$

where $[\mu_i^*]^T = \mu_i^*$. Equations (38) and (40) can be defined only if $\mathcal{H}_{\boldsymbol{x}}$ is non-singular, i.e. if the current solution point for the critical equations is not a saddle-node bifurcation (SNB) point.

Observing that and $\boldsymbol{G}_{\lambda}^i = 0$, using (33) and (40), and multiplying by μ_i^* the upper and the lower terms of the fraction in (38), one obtains:

$$\frac{d\lambda}{d\boldsymbol{a}} = -\frac{\mu_i^*\boldsymbol{G}_{\boldsymbol{a}}^i - \mu_i^*\boldsymbol{G}_{\boldsymbol{x}}^i[\mathcal{H}_{\boldsymbol{x}}]^{-1}\mathcal{H}_{\boldsymbol{a}}}{-\mu_i^*\boldsymbol{G}_{\boldsymbol{x}}^i[\mathcal{H}_{\boldsymbol{x}}]^{-1}\mathcal{H}_{\lambda}} = -\mu_i^*\boldsymbol{G}_{\boldsymbol{a}}^i - [\hat{\boldsymbol{\pi}}^*]^T\mathcal{H}_{\boldsymbol{a}}, \tag{41}$$

and, using the definition of $\mathcal{H}_{\boldsymbol{a}}$, (41) can be rewritten as follows:

$$\frac{d\lambda}{d\boldsymbol{a}} = -\mu_i^*\boldsymbol{G}_{\boldsymbol{a}}^i - [\hat{\boldsymbol{\pi}}^*]^T\mathcal{H}_{\boldsymbol{a}} = -[\boldsymbol{\pi}^*]^T\boldsymbol{H}_{\boldsymbol{a}} - [\boldsymbol{\mu}^*]^T\boldsymbol{G}_{\boldsymbol{a}}\;. \tag{42}$$

The latter equation proves that (28) applies also in the case of LIBs.

4 Case Studies

In this section, the proposed technique for computing loading margin sensitivities is applied to a 6-bus test system and to a 24-bus test system. OPF results were obtained using MATLAB [29] and GAMS-CONOPT [30], which

is a suitable solver for nonlinear programming problems and provides both primal and dual solutions.

For the sake of comparison, for the 24-bus test case, the sensitivities are also computed using a traditional numerical method as it is common practice in the literature [16]. This method is based on the continuation power flow (CPF) analysis. At this aim, UWPFLOW [31] was used.

4.1   6-bus Test Case

Figure 1 depicts the 6-bus test case that represents three generation companies (GENCOs) and three energy service companies (ESCOs). The complete set of data for this system is provided in [12].

[Figure 1 about here.]

Equality constraints $\boldsymbol{h}$ are the power flow equations and the current flows in transmission lines, as follows:

$$
\begin{aligned}
0 \;=\; & p_{Gi}^{\lambda} - p_{Li}^{\lambda} \\
& - \sum_{\iota=1}^{n_B} (v_i v_\iota B_{i\iota} \sin(\theta_i - \theta_\iota) + v_i v_\iota G_{i\iota} \cos(\theta_i - \theta_\iota)) \\
& \qquad i = 1, \ldots, n_B
\end{aligned}
\tag{43}
$$

$$
\begin{aligned}
0 \;=\; & q_{Gi} - p_{Li}^{\lambda} \tan \phi_{Li} \\
& - \sum_{\iota=1}^{n_B} (v_i v_\iota G_{i\iota} \sin(\theta_i - \theta_\iota) - v_i v_\iota B_{i\iota} \cos(\theta_i - \theta_\iota)) \\
& \qquad i = 1, \ldots, n_B
\end{aligned}
\tag{44}
$$

$$
0 \;=\; \psi_k - |j \frac{B_i}{2} v_i e^{j\theta_i} + (G_{i\iota} + jB_{i\iota})(v_i e^{j\theta_i} - v_\iota e^{j\theta_\iota})|
$$

$$k = (i, \iota) = 1, \ldots, n_L ,\qquad(45)$$

where n_B is the number of buses, n_L is the number of lines, $G_{i\iota} + jB_{i\iota} = 1/(R_{i\iota} + jX_{i\iota})$ and B_i are the series admittances and shunt susceptances, respectively, obtained from the π-model of transmission line (i, ι), the variables $\boldsymbol{\theta}$ ($\boldsymbol{\theta} \in \mathbb{R}^{n_B-1}$) and $\boldsymbol{v}$ ($\boldsymbol{v} \in \mathbb{R}^{n_B}$) are voltage angles and magnitudes, $\boldsymbol{q}_G$ ($\boldsymbol{q}_G \in \mathbb{R}^{n_B}$) are generator reactive powers,[3] $\boldsymbol{\psi}$ ($\boldsymbol{\psi} \in \mathbb{R}^{n_L}$) are current flows in transmission lines, and k_G ($k_G \in \mathbb{R}$) is a scalar variable used to distribute the system losses among generators. Thus $\boldsymbol{x} = (\boldsymbol{\theta}, \boldsymbol{v}, k_G, \boldsymbol{q}_G, \boldsymbol{\psi})$. Finally, inequalities constraints are (7)-(9).

Assuming that $\boldsymbol{a} = \boldsymbol{p} = (\boldsymbol{p}_G, \boldsymbol{p}_L)$, i.e. the parameters of the system are generator and load powers and observing that in (1)-(3) $\boldsymbol{g}$ does not depend on $\boldsymbol{p}$, one has:

$$d\lambda/d\boldsymbol{p} = -[\boldsymbol{\pi}^*]^T \boldsymbol{Hp} ,\qquad(46)$$

where

$$\boldsymbol{Hp}_{(\ell \times p)} = \left[\nabla_{\boldsymbol{p}} \boldsymbol{h}(\boldsymbol{x}^*, \lambda^*, \boldsymbol{p})\right]^T .\qquad(47)$$

Furthermore, from (6), one can rewrite (46) as follows [18]:

$$d\lambda/dp_{Gi} = -(\lambda^* + k_G^*)\pi_{pi}^*\qquad(48)$$

$$d\lambda/dp_{Li} = \lambda^* \pi_{pi}^* + (\lambda^* \tan \phi_{Li})\pi_{qi}^* ,\qquad(49)$$

where π_{pi}^* and π_{qi}^* are the Lagrangian multipliers of (43) and (44), respectively. Observe that the definition of these sensitivities is straightforward once the optimal primal and dual solutions of (1)-(3) are known.

Three simulations have been run for this 6-bus test system:

---

[3]It is assumed that there is one q_{Gi} for each bus. If no generator is connected at the bus i, then $q_{Gi}^{\max} = q_{Gi}^{\min} = 0$.

1. Without generator reactive power limits at GENCO buses, without minimum voltage limits at ESCO buses and without maximum currents in transmission lines. With these settings, the maximum loading condition is obtained at a SNB point.

2. Without minimum voltage limits at ESCO buses and without maximum currents in transmission lines. With these settings, the maximum loading condition is obtained at a LIB point.

3. With all limits included. In this case the maximum loading condition is determined by the current flow limit $\psi_{11}^{\max}$ in the transmission line from bus 5 to 6.

Table 1 gives the values of λ at the maximum loading condition for the cases described above. As it was to be expected, the more the constraints that are included in problem (1)-(3), the lower the value of λ^*.

Table 1 depicts also the values of the Lagrangian Multipliers $\boldsymbol{\mu}^*$ of inequality constraints that are binding at the maximum loading condition. At the SNB condition, there are only $n_B = 6$ binding inequality constraints.

Sensitivities with respect to inequality parameters (e.g. $\psi_k^{\max}$, $q_{Gi}^{\max}$, and $v_i^{\max}$) are straightforwardly obtained applying (28). In fact, since $\boldsymbol{h}$ does not depend on inequality parameters, the sensitivities of λ with respect to a generic parameter a_j of the inequality g_j is:

$$d\lambda/da_j = -\mu_j^* , \tag{50}$$

where μ_j is the Lagrangian multiplier associated with the inequality g_j. For example, for the SNB point:

$$d\lambda/dv_1^{\max} = -\mu_{v_{\max 1}}^* = 1.4297$$

that means that marginally increasing $v_1^{\max}$ at bus 1 would lead to an increase of the maximum loading margin λ^*. This results is reasonable, as, in general, the higher the voltage at GENCO buses, the higher the loadability of the system.

For the case that considers all limits, one has, for example:

$$d\lambda/d\psi_{11}^{\max} = -\mu_{\psi_{\max 11}}^* = 5.8466$$

that means that marginally increasing ψ_{11}^{max} in line from bus 5 to 6 would lead to an increase of the maximum loading margin λ^*. Once again, this results is also expected, as, the higher the transmission line limits, the lower the network congestion and, thus, the higher the loadability of the system.

[Table 1 about here.]

Tables 2 provides sensitivities $d\lambda/dp_{Gi}$ and $d\lambda/dp_{Li}$, which were obtained using (48) and (49). Observe that a sensitivity can be defined even if the power supply or demand at the bus is zero. If $d\lambda/dp_{Gi}$ is positive, then $d\lambda/dp_{Li}$ must be negative, since p_{Gi} is injected and p_{Li} is consumed at the same bus i.

Furthermore, $|d\lambda/dp_{Gi}| \neq |d\lambda/dp_{Li}|$ due to the way losses are handled through the variable k_G and due to the fact that loads are assumed to have constant power factor (at this regard see (48) and (49)).

Table 3 provides relevant sensitivities dv_i/dp_{Gi} and dv_i/dp_{Li}, which were obtained using (17). In particular, this table provides the sensitivities of all bus voltages with respect to p_{G1} associated with GENCO 1 and p_{L4} associated with ESCO 1 for the three cases, SNB, LIB and $\psi^{\max}$ conditions. Observe that the sensitivities with respect to the voltages that are at their limits are zero, which means that those voltages stay at their limits after applying a feasible perturbation.

Table 4 provides relevant sensitivities $d\psi_k/dp_{Gi}$ and $d\psi_k/dp_{Li}$, which were obtained using (17). In particular, Table 4 provides the sensitivities of the current flow ψ_5 from bus 2 to 4 with respect to p_{Gi} and p_{Li} at all buses.

[Table 2 about here.]

[Table 3 about here.]

[Table 4 about here.]

Table 5 illustrates the sensitivities of the loading margin λ with respect to line parameters, i.e. series resistances $R_{i\iota}$ and reactances $X_{i\iota}$, and shunt susceptances B_i. These sensitivities were obtained using (17). Observe that for SNB and LIB points, the sensitivities with respect to $R_{i\iota}$ and $X_{i\iota}$ are generally negative, while the sensitivities with respect to B_i are generally positive, hence decreasing series line parameters and increasing shunt line parameters, respectively, allows increasing λ. In the case of $\psi^{\max}$ condition, some sensitivities have opposite signs, as a consequence of transmission line congestion.

From the values of sensitivities depicted in Tables 2, 3 and 4, one can deduce that the weakest buses are likely buses 4 and 5 and that the power demand p_{L4} and p_{L5} at those buses are the parameters that mostly affect the maximum loading conditions. Observe also that the sensitivities of the loading margin λ with respect to parameters typically do not take high values. This basically means that no marginal perturbation of any parameter is able to greatly modify the loading margin of the network. Furthermore, sensitivities of Table 5 can be used to define the worst contingency, the weakest connections and/or the best locations for series and shunt compensations [17], [18] and [32]. In particular this can be useful for placing FACTS devices [16].

[Table 5 about here.]

4.2 24-bus Test Case

Figure 2 depicts the 24-bus test case, which is generally referred to as the IEEE One Area RTS-96 and is fully described in [33]. This test case is used to illustrate that the proposed technique can be easily applied to realistic size networks and that, if compared with numerical sensitivity analysis, it gives better results. At this aim, Figs. 3 and 4 illustrate respectively the sensitivities of the loading margin λ with respect to two relevant parameters, namely the power generation at bus 13 and load consumption at bus 18. In these figures, the continuous lines were obtained by solving the problem (1)-(3) several times while uniformly increasing each power supply and demand, while the stars are for the sensitivities obtained using a numerical method. In

particular a continuation power flow analysis has been used, as follows [16]:

1. The continuation power flow technique has been used for the base case parameter set and base case maximum loading margin λ_0^* obtained.

2. One parameter a is varied of a small quantity, say ϵ, and the CPF analysis is performed again. At the end of this step one has a new value of the loading margin λ_ϵ^*, and the sensitivity can be computed as follows:

$$\frac{d\lambda}{da} = \frac{\lambda_\epsilon^* - \lambda_0^*}{\epsilon} \ . \tag{51}$$

3. The previous step must be repeated for each parameter under consideration.

4. Step 1-3 must be repeated for each level of the total loading condition.

Observe that the technique proposed in this paper only needs one solution of (1)-(3) to define the sensitivities of all variables with respect of all parameters.

As it was to be expected, the higher the loading condition, the higher the absolute value of the sensitivities of the loading margin with respect to network power supply and demand. Other possible simulations are certainly possible but are beyond the aim of this paper.

[Figure 2 about here.]

[Figure 3 about here.]

[Figure 4 about here.]

5   Conclusions

This paper discusses a technique to compute sensitivities of the loading margin with respect to arbitrary parameters. The proposed technique generalizes and unifies the sensitivity formulas that have been proposed in the literature. The maximum loading condition is obtained as the solution of a OPF-problem. Hence the computation of sensitivities is accurate and computationally efficient. The proposed sensitivity formulas are illustrated and validated through two test cases.

Appendix

This appendix defines the vectors and the sub-matrices that appears in (12). Dimensions are in parenthesis.

$$\boldsymbol{F}\boldsymbol{x}_{(1\times n)} = [\nabla_{\boldsymbol{x}} f(\boldsymbol{x}^*, \lambda^*, \boldsymbol{a})]^T \tag{52}$$

$$\boldsymbol{F}_{\lambda(1\times 1)} = [\nabla_{\lambda} f(\boldsymbol{x}^*, \lambda^*, \boldsymbol{a})] \tag{53}$$

$$\boldsymbol{F}\boldsymbol{a}_{(1\times p)} = [\nabla_{\boldsymbol{a}} f(\boldsymbol{x}^*, \lambda^*, \boldsymbol{a})]^T \tag{54}$$

$$\boldsymbol{F}\boldsymbol{x}\boldsymbol{x}_{(n\times n)} = \nabla_{\boldsymbol{x}\boldsymbol{x}} f(\boldsymbol{x}^*, \lambda^*, \boldsymbol{a}) +$$
$$\sum_{l=1}^{\ell} \pi_l^* \nabla_{\boldsymbol{x}\boldsymbol{x}} h_l(\boldsymbol{x}^*, \lambda^*, \boldsymbol{a}) +$$
$$\sum_{j=1}^{m_J} \mu_j^* \nabla_{\boldsymbol{x}\boldsymbol{x}} g_j(\boldsymbol{x}^*, \lambda^*, \boldsymbol{a}) \tag{55}$$

$$\boldsymbol{F}\boldsymbol{x}_{\lambda(n\times 1)} = \nabla_{\boldsymbol{x}\lambda} f(\boldsymbol{x}^*, \lambda^*, \boldsymbol{a}) +$$
$$\sum_{l=1}^{\ell} \pi_l^* \nabla_{\boldsymbol{x}\lambda} h_l(\boldsymbol{x}^*, \lambda^*, \boldsymbol{a}) +$$

$$\sum_{j=1}^{m_J} \mu_j^* \nabla_{\boldsymbol{x}\lambda} g_j(\boldsymbol{x}^*, \lambda^*, \boldsymbol{a}) \tag{56}$$

$$\boldsymbol{F_{xa}}_{(n\times p)} = \nabla_{\boldsymbol{xa}} f(\boldsymbol{x}^*, \lambda^*, \boldsymbol{a}) +$$

$$\sum_{l=1}^{\ell} \pi_l^* \nabla_{\boldsymbol{xa}} h_l(\boldsymbol{x}^*, \lambda^*, \boldsymbol{a}) +$$

$$\sum_{j=1}^{m_J} \mu_j^* \nabla_{\boldsymbol{xa}} g_j(\boldsymbol{x}^*, \lambda^*, \boldsymbol{a}) \tag{57}$$

$$\boldsymbol{F_{\lambda x}}_{(1\times n)} = \nabla_{\lambda\boldsymbol{x}} f(\boldsymbol{x}^*, \lambda^*, \boldsymbol{a}) +$$

$$\sum_{l=1}^{\ell} \pi_l^* \nabla_{\lambda\boldsymbol{x}} h_l(\boldsymbol{x}^*, \lambda^*, \boldsymbol{a}) +$$

$$\sum_{j=1}^{m_J} \mu_j^* \nabla_{\lambda\boldsymbol{x}} g_j(\boldsymbol{x}^*, \lambda^*, \boldsymbol{a}) \tag{58}$$

$$\boldsymbol{F_{\lambda\lambda}}_{(1\times 1)} = \nabla_{\lambda\lambda} f(\boldsymbol{x}^*, \lambda^*, \boldsymbol{a}) +$$

$$\sum_{l=1}^{\ell} \pi_l^* \nabla_{\lambda\lambda} h_l(\boldsymbol{x}^*, \lambda^*, \boldsymbol{a}) +$$

$$\sum_{j=1}^{m_J} \mu_j^* \nabla_{\lambda\lambda} g_j(\boldsymbol{x}^*, \lambda^*, \boldsymbol{a}) \tag{59}$$

$$\boldsymbol{F_{\lambda a}}_{(1\times p)} = \nabla_{\lambda\boldsymbol{a}} f(\boldsymbol{x}^*, \lambda^*, \boldsymbol{a}) +$$

$$\sum_{l=1}^{\ell} \pi_l^* \nabla_{\lambda\boldsymbol{a}} h_l(\boldsymbol{x}^*, \lambda^*, \boldsymbol{a}) +$$

$$\sum_{j=1}^{m_J} \mu_j^* \nabla_{\lambda\boldsymbol{a}} g_j(\boldsymbol{x}^*, \lambda^*, \boldsymbol{a}) \tag{60}$$

$$\boldsymbol{H_x}_{(\ell\times n)} = [\nabla_{\boldsymbol{x}} \boldsymbol{h}(\boldsymbol{x}^*, \lambda^*, \boldsymbol{a})]^T \tag{61}$$

$$\boldsymbol{H_\lambda}_{(\ell\times 1)} = [\nabla_{\lambda} \boldsymbol{h}(\boldsymbol{x}^*, \lambda^*, \boldsymbol{a})]^T \tag{62}$$

$$\boldsymbol{H_a}_{(\ell\times p)} = [\nabla_{\boldsymbol{a}} \boldsymbol{h}(\boldsymbol{x}^*, \lambda^*, \boldsymbol{a})]^T \tag{63}$$

$$\boldsymbol{G_x}_{(m_J\times n)} = [\nabla_{\boldsymbol{x}} \boldsymbol{g}(\boldsymbol{x}^*, \lambda^*, \boldsymbol{a})]^T \tag{64}$$

$$\boldsymbol{G_\lambda}_{(m_J\times 1)} = [\nabla_{\lambda} \boldsymbol{g}(\boldsymbol{x}^*, \lambda^*, \boldsymbol{a})]^T \tag{65}$$

$$\boldsymbol{G_a}_{(m_J\times p)} = [\nabla_{\boldsymbol{a}} \boldsymbol{g}(\boldsymbol{x}^*, \lambda^*, \boldsymbol{a})]^T \ . \tag{66}$$

References

[1] Chiang, H.- D., Dobson, I, Thomas, R. J., Thorp, J. S., and Fekih-Ahmed, L.: 'On Voltage Collapse in Electric Power System,' *IEEE Transactions on Power Systems*, 1990, **5**, pp. 601-611.

[2] Van Cutsem, T., and Vournas, C. *Voltage Stability of Electric Power Systems*. Boston: Kluwer International Series in Engineering & Computer Science, 1998.

[3] Cañizares, C. A.: 'Voltage Stability Assessment: Concepts, Practices and Tools,' IEEE/PES Power System Stability Subcommittee, Final Document, Tech. Rep. SP101PSS_2002, 2002, available at http://www.power.uwaterloo.ca.

[4] Dobson, I.: 'Observations on the Geometry of Saddle Node Bifurcation and Voltage Collapse in Electrical Power Systems,' *IEEE Transactions on Circuits and Systems - I: Fundamental Theory and Applications*, 1992, **39**, (3), pp. 240-243.

[5] Dobson, I., and Lu, L.: 'Voltage Collapse Precipitated by the Immediate Change of Stability when Generator Reactive Power Limits are Encountered,' *IEEE Transactions on Circuits and Systems - I: Fundamental Theory and Applications*, 1992, **39**, (9), pp. 762-766.

[6] Cañizares, C. A., Alvarado, F. L., DeMarco, C. L. I. Dobson, and Long, W. F.: 'Point of Collapse Method Applied to AC/DC Power Systems,' *IEEE Transactions on Power Systems*, 1992, **7**, (2), pp. 673-683.

[7] Ajjarapu, V., and Christy, C.: 'The Continuation Power Flow: a Tool for Steady State Voltage Stability Analysis,' *IEEE Transactions on Power Systems*, 1992, **7**, pp. 416-423.

[8] Cañizares, C. A.: 'Applications of Optimization to Voltage Collapse Analysis,' in *IEEE-PES Summer Meeting*, 1998, (San Diego, USA).

[9] Van Cutsem, T.: 'A Method to compute Reactive Power Margins with respect to Voltage Collapse,' in *IEEE Transactions on Power Systems*, 1991, **6**, pp. 145-156.

[10] Cañizares, C. A., Rosehart, W., Berizzi, A., and Bovo, C.: 'Comparison of Voltage Security Constrained Optimal Power Flow Techniques,' in *Proc. 2001 IEEE-PES Summer Meeting*, 2001, (Vancouver, BC, Canada).

[11] Rosehart, W. D., Cañizares, C. A., and Quintana, V.: 'Multi-Objective Optimal Power Flows to Evaluate Voltage Security Costs in Power Networks,' *IEEE Transactions on Power Systems*, 2003, **18**, (2), pp. 578-587.

[12] Milano, F., Cañizares, C. A., and Invernizzi, M.: 'Multi-objective Optimization for Pricing System Security in Electricity Markets,' *IEEE Transactions on Power Systems*, 2003, **18**, (2).

[13] Cañizares, C. A.: 'Calculating Optimal System Parameters to Maximize the Distance to Saddle-Node Bifurcations,' *IEEE Transactions on Circuits and Systems - I: Fundamental Theory and Applications*, 1998, **45**, (3), pp. 225-237.

[14] Begović, M. M., and Phadke, G.: 'Control of Voltage Stability using Sensitivity Analysis,' *IEEE Transactions on Power Systems*, 1992, **7**, (1), pp. 114-120.

[15] Greene, S., Dobson, I., and Alvarado, F. L.: 'Sensitivity of the Loading Margin to Voltage Collapse with Respect to Arbitrary Parameters,' *IEEE Transactions on Power Systems*, 1997, **12**, (1), pp. 262-272.

[16] Cañizares, C. A., Cavallo, C., Pozzi, M. and Corsi, S.: 'Comparing Secondary Voltage Regulation and Shunt Compensation for Improving Voltage Stability and Transfer Capability in the Italian Power System,' *Electric Power Systems Research*, 2005, **73**, (2), pp. 67-76.

[17] Greene, S., Dobson, I., and Alvarado, F. L.: 'Contingency Ranking for Voltage Collapse via Sensitivities from Single Nose Curve,' *IEEE Transactions on Power Systems*, 1999, **14**, (1), pp. 232-240.

[18] Milano, F., Cañizares, C. A., and Invernizzi, M.: 'Voltage Stability Constrained OPF Market Models Considering N-1 Contingency Criteria,' *Electric Power Systems Research*, 2005, **74**, (1), pp. 27-36.

[19] Flueck, A. J., Gonella, R., and Dondeti, J.: 'A New Power Sensitivity Method of Ranking Branch Contingencies for Voltage Collapse,' *IEEE Transactions on Power Systems*, 2002, **17**, (2), pp. 265-270.

[20] Greene, S., Dobson, I., and Alvarado, F. L.: 'Sensitivity of Transfer Capability Margins with a Fast Formula,' *IEEE Transactions on Power Systems*, 2002, **17**, (1), pp. 34-40.

[21] Capitanescu, F., and Van Cutsem, T.: 'Unified Sensitivity Analysis of Unstable or Low Voltages Caused by Load Increases or Contingencies,' *IEEE Transactions on Power Systems*, 2005, **20**, (1), pp. 321-329.

[22] Orfanogianni, T., and Bacher, R.: 'Steady-state Optimization in Power Systems with Series FACTS Devices,' *IEEE Transactions on Power Systems*, 2003, **18**, (1), pp. 19-26.

[23] Fiacco, A. V.: *Introduction to Sensitivity Analysis in Nonlinear Programming.* Academic Press, 1983, (New York, USA).

[24] Castillo, E., Conejo, A. J., Castillo, C., Mínguez, R., and Ortigosa, D.: 'Perturbation Approach to Sensibility Analysis in Mathematical Programming,' *Journal of Optimization Theory and Applications*, 2006, **128**, (1), pp. 49-74.

[25] Conejo, A. J., Castillo, E., Mínguez, R., and Milano, F.: 'Locational Marginal Price Sensitivities,' *IEEE Transactions on Power Systems*, 2005, **20**, (4), pp. 2026-2033.

[26] Xie, K., Song, Y.-H., Stonham, J., Yu, E., and Liu, G.: 'Decomposition Model and Interior Point Methods for Optimal Spot Pricing of Electricity in Deregulation Environments,' *IEEE Transactions on Power Systems*, 2000, **15**, (1), pp. 39-50.

[27] Luenberger, D. G.: *Linear and Nonlinear Programming, 2nd ed.* Reading, MA: Addison-Wesley, 1989.

[28] Bazaraa, M. S., Sherali, H. D., and Shetty, C. M.: *Nonlinear Programming, Theory and Algorithms, 2nd ed.* Wiley, 1993, (New York, USA).

[29] The MathWorks, Inc., 'Matlab Programming,' 2005, available at http://www.mathworks.com.

[30] A. S. Drud, A. S.: *GAMS/CONOPT*, ARKI Consulting and Development.

[31] Cañizares, C. A. et al.:, 'UWPFLOW Program', 2000, (University of Waterloo), available at http://www.power.uwaterloo.ca.

[32] Capitanescu, F., and Van Cutsem, T.: 'Preventive Control of Voltage Security Margins: A Multicontingency Sensitivity-based Approach,' *IEEE Transactions on Power Systems*, 2002, **17**, (2), pp. 358-364.

[33] Reliability Test System Task Force of the Application of Probability Methods subcommittee:,'The IEEE Reliability Test System - 1996,' *PES*, 1999, **14**, (3), pp. 1010-1020.

List of Figures

Figure 1: 6-bus test system.
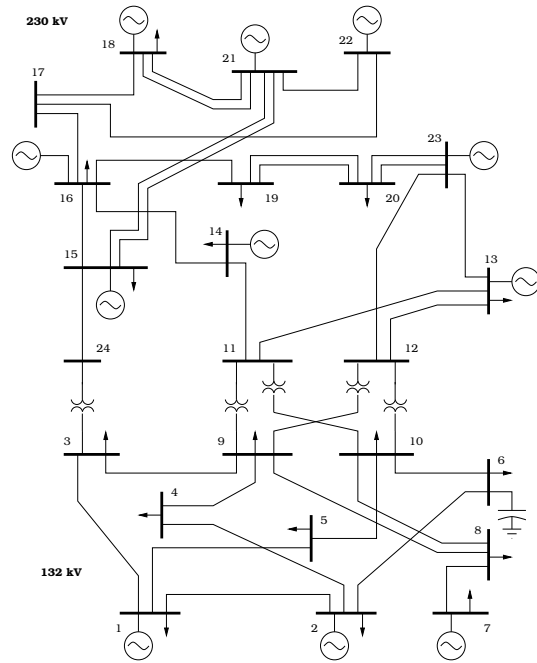
Figure 2: 24-bus test system (IEEE One Area RTS-96 [33]).
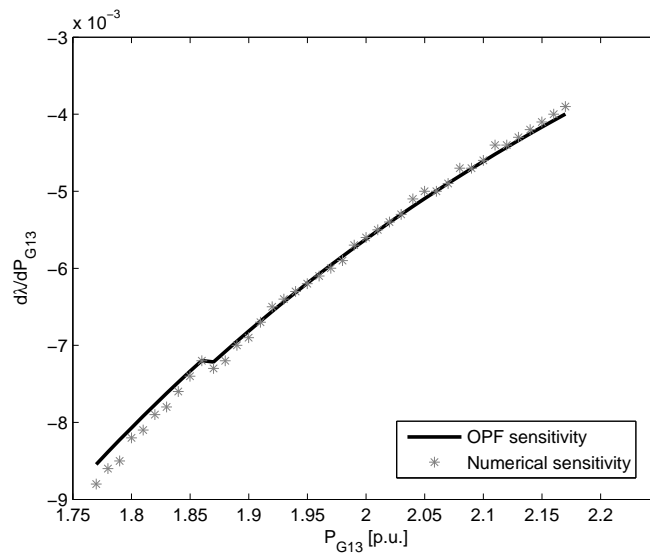
Figure 3: Sensitivity $d\lambda/dP_G$ at bus 13 for the 24-bus test system.
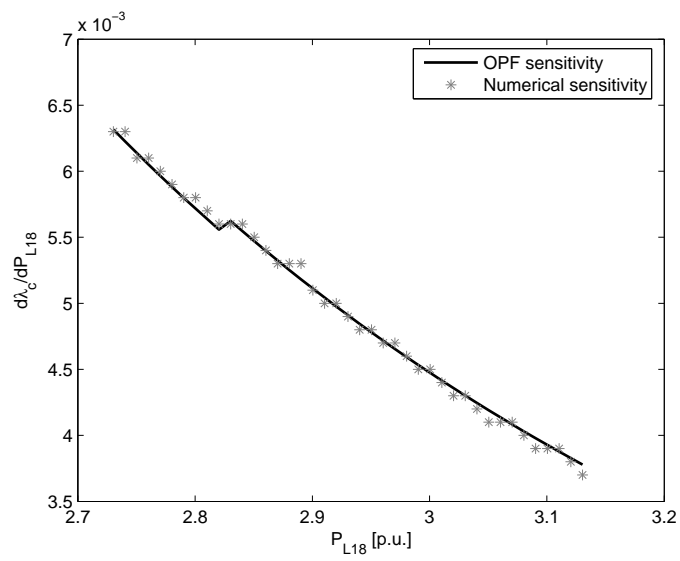
Figure 4: Sensitivity $d\lambda/dP_L$ at bus 18 for the 24-bus test system.

List of Tables

Table 1: Lagrangian Multipliers $\boldsymbol{\mu}^*$ at Different Maximum Loading Conditions for the 6-bus test system.

SNB $\lambda^* = 2.7509$		LIB $\lambda^* = 1.7557$		$\psi^{\max}$ $\lambda^* = 1.3711$	
μ_j^*	Active g_j	μ_j^*	Active g_j	μ_j^*	Active g_j
-1.4297	$v_1^{\max}$	-1.4424	$v_1^{\max}$	3.9339	$v_5^{\min}$
-2.1552	$v_2^{\max}$	-0.1519	$q_{G1}^{\max}$	-3.2094	$v_1^{\max}$
-1.6549	$v_3^{\max}$	-0.2529	$q_{G2}^{\max}$	-2.3286	$v_2^{\max}$
-0.1139	$q_{G4}^{\max}$	-0.2608	$q_{G3}^{\max}$	0.2970	$q_{G6}^{\min}$
-0.4482	$q_{G5}^{\max}$	-0.3079	$q_{G4}^{\max}$	-0.1280	$q_{G4}^{\max}$
-0.0724	$q_{G6}^{\max}$	-0.3480	$q_{G5}^{\max}$	-0.8252	$q_{G5}^{\max}$
-	-	-0.3087	$q_{G6}^{\max}$	-5.8466	$\psi_{11}^{\max}$

Table 2: Sensitivities $d\lambda/dp_{G_j}$ and $d\lambda/dp_{L_j}$ for the 6-bus test system.

Bus	SNB		LIB		ψ^{max}	
i	$\frac{d\lambda}{dp_{Gi}}$	$\frac{d\lambda}{dp_{Li}}$	$\frac{d\lambda}{dp_{Gi}}$	$\frac{d\lambda}{dp_{Li}}$	$\frac{d\lambda}{dp_{Gi}}$	$\frac{d\lambda}{dp_{Li}}$
1	-0.0242	0.0187	-0.0655	0.0599	0.0042	-0.0039
2	-0.0114	0.0089	-0.0004	0.0004	0.0031	-0.0030
3	0.0508	-0.0393	0.0745	-0.0682	-0.0112	0.0105
4	0.2697	-0.4175	0.1652	-0.5116	0.0792	-0.1916
5	1.2487	-1.8289	0.2671	-0.6721	0.5088	-1.2711
6	0.2186	-0.2355	0.2278	-0.3891	-0.0948	0.2250

Table 3: Relevant sensitivities dv_i/dp_{G_i} and dv_i/dp_{L_i} for the 6-bus test system.

Bus	SNB		LIB		$\psi^{\max}$	
i	$\frac{dv_i}{dp_{G1}}$	$\frac{dv_i}{dp_{L4}}$	$\frac{dv_i}{dp_{G1}}$	$\frac{dv_i}{dp_{L4}}$	$\frac{dv_i}{dp_{G1}}$	$\frac{dv_i}{dp_{L4}}$
1	0	0	0	0	0	0
2	0	0	-0.0370	0.0176	0	0
3	0	0	-0.0377	0.0767	-0.0020	-0.0147
4	0.0235	-0.5344	-0.0166	-0.0828	0.0044	-0.0937
5	0.0029	-0.0044	-0.0256	0.1007	0	0
6	0.0005	0.0374	-0.0368	0.1001	-0.0020	0.0013

Table 4: Relevant sensitivities $d\psi_k/dp_{G_j}$ and $d\psi_k/dp_{L_j}$ for the 6-bus test system.

Bus	SNB		LIB		ψ^{max}	
i	$\frac{d\psi_{11}}{dp_{Gi}}$	$\frac{d\psi_{11}}{dp_{Li}}$	$\frac{d\psi_{11}}{dp_{Gi}}$	$\frac{d\psi_{11}}{dp_{Li}}$	$\frac{d\psi_{11}}{dp_{Gi}}$	$\frac{d\psi_{11}}{dp_{Li}}$
1	-0.5411	0.4168	-0.3596	0.3290	-0.2012	0.1894
2	0.1952	-0.1518	0.1410	-0.1290	0.1022	-0.0962
3	0.2061	-0.1558	0.1137	-0.1040	0.0155	-0.0146
4	-3.9624	5.0434	-1.0240	0.9958	-0.7429	0.9555
5	3.1995	-4.6362	0.1195	-0.5509	0.4206	-1.1872
6	0.6392	-0.6363	0.2997	-0.4902	-0.0606	0.1883

Table 5: Sensitivities $d\lambda/dR_{i\iota}$, $d\lambda/dX_{i\iota}$ and $d\lambda/dB_i$ for the 6-bus test system.

	SNB	$\lambda^* = 2.7509$		
Line k	from - to i-ι	$d\lambda/dR_{i\iota}$	$d\lambda/dX_{i\iota}$	$d\lambda/dB_i$
1	1-2	-0.0053	-0.0052	0
2	1-4	-0.5405	-0.8568	0.0243
3	1-5	-1.2488	-1.5071	0.0611
4	2-3	-0.0155	-0.0335	0
5	2-4	-2.3442	-2.1009	0.0243
6	2-6	-0.5493	-0.3639	0.0238
7	2-5	-1.1183	-1.3871	0.0611
8	3-5	-1.3456	-1.4712	0.0611
9	3-6	-1.1838	-1.6511	0.0238
10	4-5	-0.1462	-0.0872	0.0854
11	5-6	-0.1201	-0.6340	0.0849

	LIB	$\lambda^* = 1.7557$		
Line k	from - to i-ι	$d\lambda/dR_{i\iota}$	$d\lambda/dX_{i\iota}$	$d\lambda/dB_i$
1	1-2	-0.0750	-0.0222	0.2153
2	1-4	-0.3084	-0.6687	0.1958
3	1-5	-0.2700	-0.4369	0.2036
4	2-3	-0.0221	-0.0150	0.2693
5	2-4	-0.0957	-0.6986	0.2436
6	2-6	-0.1850	-0.2492	0.2614
7	2-5	-0.0604	-0.1872	0.2515
8	3-5	-0.0462	-0.1389	0.2576
9	3-6	-0.0774	-0.6610	0.2676
10	4-5	-0.0107	-0.0023	0.2319
11	5-6	0.0022	-0.0076	0.2498

	$\psi^{\max}$	$\lambda^* = 1.3711$		
Line k	from - to i-ι	$d\lambda/dR_{i\iota}$	$d\lambda/dX_{i\iota}$	$d\lambda/dB_i$
1	1-2	0.0003	0.0003	0
2	1-4	-0.3657	-0.3221	0.0547
3	1-5	-1.3891	-0.9993	0.3342
4	2-3	-0.0019	0.0071	0
5	2-4	-1.3654	-0.6394	0.0547
6	2-6	0.9754	0.1581	-0.1354
7	2-5	-1.2424	-0.8746	0.3342
8	3-5	-1.2444	-0.6814	0.3342
9	3-6	2.6654	1.2152	-0.1354
10	4-5	-0.1468	-0.0063	0.3889
11	5-6	0.2990	0.6228	-0.8207